Simultaneous Generation of X-ray and Range Images using XCAT under Motion

Oleksiy Rybakov, Bastian Bier, Jennifer Maier, Mathias Unberath and Andreas Maier

***Abstract*—Novel algorithms in the field of X-ray imaging are commonly evaluated on simulation software first, before they are implemented on a clinical scanner in order to test their performance in a very controlled setup. This reduces patient dose and facilitates the development of new approaches and methods. In recent years, range imaging applications were established in the field of medical imaging. Range imaging showed its potential in radiotherapy, augmented reality, and, recently, also for motion correction in cone-beam computed tomography.**

In this work, we present an open-source software tool that allows to generate X-ray projections and surface information in one step completely on the graphics processing unit. To this end, we extend a state-of-the-art rendering method based on an append buffer. Arbitrary imaging geometries for the X-ray source and the range imaging camera can be selected. We test the proposed method on the XCAT phantom in two fundamentally different scenarios: a weight-bearing acquisition showing a squat, and a supine acquisition of a breathing patient.

I. Introduction

In recent years, significant achievements to improve image quality and dose reduction in X-ray imaging have been accomplished. Today's scanners expose patients to only a limited amount of radiation [1], [2]. In the development process, computationally expensive simulations using phantoms [3] are commonly used to simplify the evaluation of novel algorithms.

One category of these new algorithms is based on depth cameras, which have been established in the last years in the field of medical imaging such as augmented reality [4], motion estimation in SPECT imaging [5], and radiotherapy [6]. Moreover, range imaging has recently been tested in the scenario of imaging under weight-bearing conditions [7] and of a breathing patient [8] to estimate patient motion. In order to facilitate research in these areas, there is a demand for software that is able to simulate range imaging and the corresponding X-ray projections simultaneously.

In this work, we present an open-source software tool based on the CONRAD framework [9][1] that allows to generate X-ray projections and to obtain surface data completely on the graphics processing unit (GPU) in one step. To this end, we extend a method proposed by Maier et al. [10], where X-ray projections of objects defined as spline-based surfaces are rendered using an append buffer structure. The software allows to use independent and arbitrary trajectories for the X-ray system and the depth camera. Furthermore, we can integrate a motion field to simulate patient motion and capture X-ray and surface data in the same motion state. We tested our method in two scenes based on the XCAT phantom [11]: a) squatting knees and b) breathing.

O. Rybakov, B. Bier, J. Maier, M. Unberath and A. Maier are with the Department of Computer Science, Pattern Recognition Lab, Friedrich-Alexander-University Erlangen-Nuremberg, Erlangen, Germany.

[1]http://conrad.stanford.edu/

II. Materials and Methods

The Append Buffer Structure: The projection of complex realistic phantom models requires high computational effort, since many common graphics acceleration algorithms cannot be applied to this task. To overcome this drawback, Maier et al. [10] proposed a different graphics pipeline that simulates transmission projections for CT reconstruction using moving spline surface models. The complete processing pipeline is devised to run on the GPU only. First, a 3D point cloud is generated to sample the surface of each image object. Afterwards, neighboring points are tesselated by connecting them to triangles to deliver an approximation of the analytic surface shape. Then, the points are projected onto the detector plane using an affine transform to project triangles onto triangles in detector coordinates. For each pixel, intersections are stored in an append buffer and sorted with respect to their depth. Finally, for each segment along the ray, an absorption model is evaluated on the traversed object, considering its material dependent attenuation coefficient.

Extension to Extract Surface Data: In this work, we present an extension of this pipeline. Instead of ordering intersections along their depth, we can also look for the intersection with the smallest depth for each pixel and store this depth in a second frame. This value represents the surface point visible from the current camera position. Using this information, we can generate X-ray projections and obtain surface information of the object of interest on the GPU in one step. The depth of the surface information is implemented to an accuracy of 0.1 μm. Furthermore, our tool supports surface extraction for arbitrary detector sizes, detector spacings and camera viewpoints.

Point Cloud Generation: Using the depth value d of the depth image at each detector pixel $\boldsymbol{x}_{\text{pixel}} \in \mathbb{R}^3$, a corresponding 3D surface point cloud can be computed using the known camera geometry:

$$\boldsymbol{x}_{\text{surface}} = \boldsymbol{x}_{\text{camera}} + d \cdot \frac{\boldsymbol{x}_{\text{pixel}} - \boldsymbol{x}_{\text{camera}}}{||\boldsymbol{x}_{\text{pixel}} - \boldsymbol{x}_{\text{camera}}||_2}, \qquad (1)$$

where $\boldsymbol{x}_{\text{surface}} \in \mathbb{R}^3$ denotes the surface point and $\boldsymbol{x}_{\text{camera}} \in \mathbb{R}^3$ is the camera origin. Please note that $\boldsymbol{x}_{\text{pixel}}$, $\boldsymbol{x}_{\text{camera}}$, and $\boldsymbol{x}_{\text{surface}}$ are represented in world coordinates.

III. Experiments and Results

Set-Up: We test our approach on the XCAT phantom performing a single squat between 60° and 90° flexion angle.

This scenario is motivated by the rising interest in acquisitions under weight-bearing conditions [7], [12]. To animate the XCAT model in a realistic, yet simple way for squatting patients, we separate squatting into a rigid bone motion and a non-rigid soft-tissue motion. Using the positions of joint centers for both knees, ankles and hips we can describe bone motion completely. Then, soft-tissue motion can be modeled by deforming the B-spline motion model. Additionally, we look at the thorax of a breathing XCAT torso. All experiments are simulated as cone-beam computed tomography short scans acquiring 248 projections with a detector size of 620×480 pixels of size of 1 mm×1 mm.

Results: Figure 1 shows the results for a squatting patient. The top, central and bottom lines depict a patient at a knee flexion angle $\varphi_K = 90°$, 75° and 60°, respectively. The left column depicts X-ray projections, the central column the surface of the patient's lower body and the right column shows the surface as a point cloud. Please note that the point clouds appear truncated due to the limited field of view of the camera.

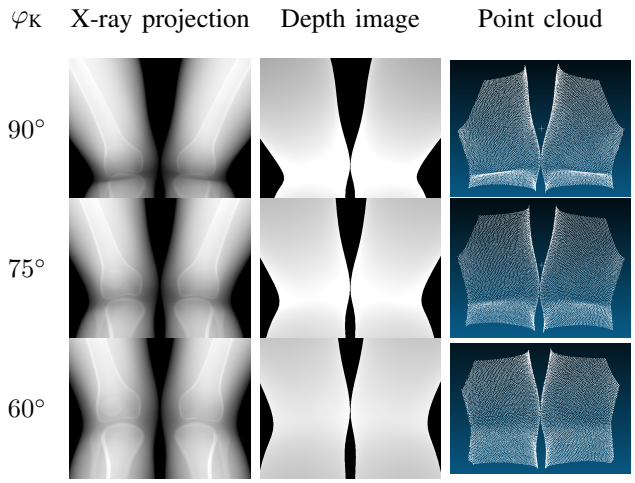

Fig. 1. X-ray projections, depth images and point clouds of a squatting patient for different motion states.

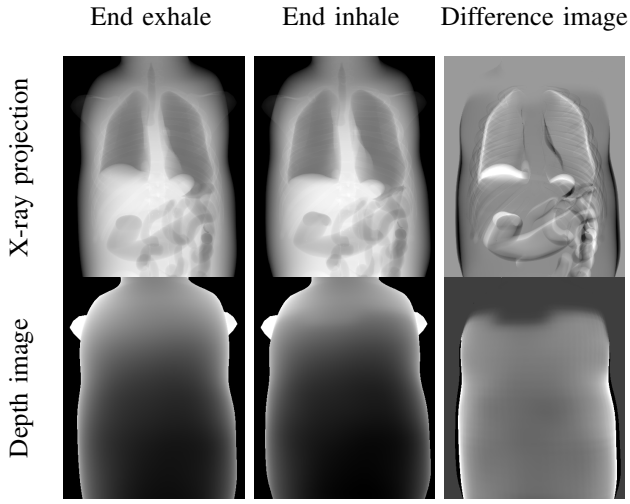

Fig. 2. X-ray projections and depth images of a thorax during breathing.

Figure 2 shows the resulting images for the breathing torso. The X-ray source and the depth camera are located anterior to the patient. We show the two motion states at end exhale and end inhale in the left and central column, respectively. In order to visualize the movement in the images more clearly, the difference between both states is depicted on the right.

IV. Discussion and Conclusion

We devised an open-source software tool that runs completely on the GPU and enables simultaneous generation of X-ray projections and surface information of the patient's entire body. Moreover, a point cloud representing the surface of the patient's body can be reconstructed using the depth and detector information. By applying a motion field, we can simulate a dynamic scene that proves beneficial for the investigation of acquisitions under weight-bearing conditions, such as squatting, or other sources of intra-scan motion, such as respiration.

One limitation of the simulated depth camera is that no physical sources of errors are modeled. On the other hand, noise, sensor drift and multipath effects are commonly present in real acquisitions. However, these effects can still be added to the depth image. In particular, this is the case as we also know the material of the closest intersection point. In the future, more realistic depth image acquisition is going to be investigated by considering the material properties of the tracked surface. Furthermore, other effects present in the clinical environment like partial occlusion from the table or other instruments have to be considered.

Nevertheless, our work facilitates future research in the field of range imaging in combination with cone-beam computed tomography, for instance in imaging under weight-bearing conditions or radiotherapy.

References

[1] R. Fahrig, R. Dixon, T. Payne, R. L. Morin, A. Ganguly, and N. Strobel, "Dose and image quality for a cone-beam c-arm ct system," *Med. Phys.*, vol. 33, no. 12, pp. 4541–4550, 2006.

[2] J. Hausleiter, T. Meyer, M. Hadamitzky, E. Huber, M. Zankl, S. Martinoff, A. Kastrati, and A. Schömig, "Radiation dose estimates from cardiac multislice computed tomography in daily practice," *Circulation*, vol. 113, no. 10, pp. 1305–1310, 2006.

[3] L. A. Shepp and B. F. Logan, "The fourier reconstruction of a head section," *IEEE Trans. Nucl. Sci.*, vol. 21, no. 3, pp. 21–43, 1974.

[4] M. Fischer, B. Fuerst, S. C. Lee, J. Fotouhi, S. Habert, S. Weidert, E. Euler, G. Osgood, and N. Navab, "Preclinical usability study of multiple augmented reality concepts for k-wire placement," *IJCARS*, vol. 11, no. 6, pp. 1007–1014, 2016.

[5] J. E. McNamara, P. H. Pretorius, K. Johnson, J. M. Mukherjee, J. Dey, M. A. Gennert, and M. A. King, "A flexible multicamera visual-tracking system for detecting and correcting motion-induced artifacts in cardiac spect slices," *Med. Phys.*, vol. 36, no. 5, pp. 1913–1923, 2009.

[6] T. Geimer, M. Unberath, O. Taubmann, C. Bert, and A. Maier, "Combination of markerless surrogates for motion estimation in radiation therapy," in *CARS*, 2016.

[7] B. Bier, M. Unberath, T. Geimer, J. Maier, G. Gold, M. Levenston, R. Fahrig, and A. Maier, "Motion Compensation using Range Imaging in C-arm Cone-Beam CT," in *MIUA 2017*, 2017.

[8] O. Taubmann, J. Wasza, C. Forman, P. Fischer, J. Wetzl, A. Maier, and J. Hornegger, "Prediction of respiration-induced internal 3-d deformation fields from dense external 3-d surface motion," in *Proc. 28th Int. Congr. Exhib.*, pp. 33–34, 2014.

[9] A. Maier, H. G. Hofmann, M. Berger, P. Fischer, C. Schwemmer, H. Wu, K. Müller, J. Hornegger, J.-H. Choi, C. Riess, *et al.*, "Conrad - a software framework for cone-beam imaging in radiology," *Med. Phys.*, vol. 40, no. 11, 2013.

[10] A. Maier, H. G. Hofmann, C. Schwemmer, J. Hornegger, A. Keil, and R. Fahrig, "Fast simulation of x-ray projections of spline-based surfaces using an append buffer," *Phys. Med. Biol.*, vol. 57, no. 19, p. 6193, 2012.

[11] W. Segars, G. Sturgeon, S. Mendonca, J. Grimes, and B. M. Tsui, "4d xcat phantom for multimodality imaging research," *Med. Phys.*, vol. 37, no. 9, pp. 4902–4915, 2010.

[12] J.-H. Choi, R. Fahrig, A. Keil, T. F. Besier, S. Pal, E. J. McWalter, G. S. Beaupré, and A. Maier, "Fiducial marker-based correction for involuntary motion in weight-bearing c-arm ct scanning of knees. part i. numerical model-based optimization," *Med. Phys.*, vol. 40, no. 9, 2013.